13. Stoeckel, K., Schwab, M. & Thoenen, H. *Brain Res.* **89,** 1–14 (1974).
14. Angeletti, R. H. & Bradshaw, R. A. *Proc. natn. Acad. Sci. U.S.A.* **68,** 2417–2420 (1971).
15. Scott, J. *et al. Nature* **302,** 538–540 (1983).
16. Ullrich, A., Gray, A., Berman, C. & Dull, T. J. *Nature* **303,** 821–825 (1983).
17. Darling, T. L. J. *et al. Cold Spring Harb. Symp. quant. Biol.* **48,** 427–434 (1983).
18. Menescini-Chen, M. G., Chen, J. S. & Levi-Montalcini, R. *Archs ital. Biol.* **116,** 53–84 (1978).
19. Letourneau, P. C. *Devl Biol.* **66,** 183–196 (1978).
20. Gundersen, R. W. & Barrett, J. N. *Science* **206,** 1079–1080 (1979).
21. Levi-Montalcini, R. *Prog. Brain Res.* **45,** 235–258 (1976).
22. Renehan, W. E. & Munger, B. L. *J. comp. Neurol.* **246,** 129–145 (1986).
23. Iggo, A. *Br. med. Bull.* **33,** 97–102 (1977).
24. Iggo, A. & Andres, K. H. *A. Rev. Neurosci.* **5,** 1–31 (1982).
25. Davies, A. M. & Lumsden, A. G. S. *J. comp. Neurol.* **223,** 124–137 (1984).
26. Davies, A. M. & Lumsden, A. G. S. *J. comp. Neurol.* **253,** 13–24 (1986).
27. Korsching, S. & Thoenen, H. *Proc. natn. Acad. Sci. U.S.A.* **80,** 3513–3516 (1983).
28. Bandtlow, C., Heumann, R., Schwab, M. & Thoenen, H. *EMBO J.* (in the press).
29. Rush, R. A. *Nature* **312,** 364–367 (1984).
30. Finn, P. J., Ferguson, I. A., Renton, F. J. & Rush, R. A. *J. Neurocytol.* **15,** 169–176 (1986).
31. Lumsden, A. G. S. & Davies, A. M. *Nature* **306,** 786–788 (1983).
32. Lumsden, A. G. S. & Davies, A. M. *Nature* **323,** 538–539 (1986).
33. Lowry, O. H., Rosenbrough, N. J., Farr, A. L. & Randall, R. J. *J. biol. Chem.* **193,** 265–275 (1951).

Three-dimensional structure of a complex of antibody with influenza virus neuraminidase

P. M. Colman, W. G. Laver*, J. N. Varghese, A. T. Baker, P. A. Tulloch, G. M. Air† & R. G. Webster‡

CSIRO Division of Protein Chemistry, 343 Royal Parade, Parkville, 3052, Australia
* John Curtin School of Medical Research, Australian National University, Canberra 2601, Australia
† Department of Microbiology, University of Alabama, Birmingham, Alabama 35294, USA
‡ St Jude Children's Research Hospital, Memphis, Tennessee 38101, USA

The structure of a complex between influenza virus neuraminidase and an antibody displays features inconsistent with the inflexible 'lock and key' model of antigen–antibody binding. The structure of the antigen changes on binding, and that of the antibody may also change; the interaction therefore has some of the character of a handshake.

WE report here the first analysis by X-ray diffraction of the three-dimensional structure of a viral antigen complexed with an antibody Fab fragment. The antigen is the influenza virus enzyme neuraminidase (reviewed in ref. 1).

Sufficient data on the chemical[2] and spatial[3–6] structure of antibodies emerged in the 1970s to provide a basis for understanding how variation in antibody structure occurs, but the question of how different antibodies accommodate different macromolecular epitopes remains unresolved. The antigen binding fragments (Fab) of immunoglobulins consist of a light chain (L) and the N-terminal half of the heavy (H) chain. On each chain there are two globular domains of ~100 amino acids, the N-terminal domain in each chain being variable (V_L and V_H) and the C-terminal domain conserved (C_L and C_H1) in their amino-acid sequences. V_L and V_H domains are associated with each other, forming a variable module and C_L and C_H1 form the constant module. Three complementarity-determining regions (CDR1, 2 and 3) from each of the V_L and V_H domains are clustered at the extremity of the Fab arms, and they determine the binding specificity of an immunoglobulin molecule.

The three-dimensional structures of five free Fab fragments[7–11] and one in complex with lysozyme[12] have been reported. Four of the structures, New[7], Kol[8], McPC603[9] and J539[10], are well refined and form the basis of the following generalizations which also appear valid for the other two, S10/1 (ref. 11) and D1.3 (ref. 12). The pairing of V_L and V_H domains is determined by amino acids from both the framework region and the CDRs. Most of the surface area buried in the interface derives from conserved residues and this observation explains the largely conserved geometry of V_L–V_H pairing[13]. Small differences in pairing presumably result from interactions among the CDR amino acids[14]. Analysis of the V_L–V_H contact surface shows it to be unlike other interfaces between β-sheets[15]. Amino acids from the outermost strands of the two sheets fold into the interface where they contribute the bulk of the buried surface. C_L–C_H1 dimers are similarly conserved in their association pattern[16]. More variable is the so-called elbow angle[17,18]

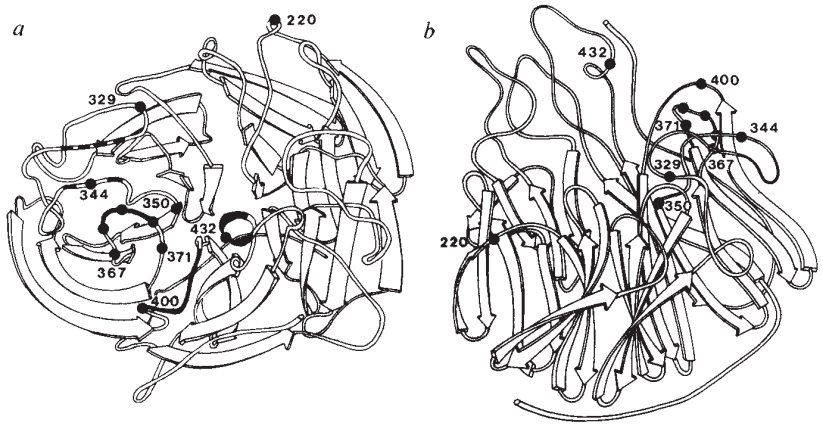

Fig. 1 Schematic diagrams of chain fold in N2 and N9 neuraminidase viewed down the 4-fold axis (*a*) and perpendicular to this axis (*b*). The symmetry axis is bottom right in *a* and standing vertical at the left rear in *b*. The view of the neuraminidase in *b* is similar to that shown in Fig. 5. Tagged residues and adjacent chain segments are referred to in the text. N2 numbering is used. In *a*, the side chains of amino acids 368–370 point towards the viewer, whilst that of Arg 371 points away and into the catalytic site located above and to the right of C_α 371. Mutations at positions 367, 369, 370, 400, and 432, as detailed in Fig. 2, abolish the binding of NC41 antibody to neuraminidase, whereas mutations at 368 and 329 reduce that binding. A mutation at 220, which falls outside the NC41 epitope, has no effect on NC41 binding to neuraminidase (see Fig. 2). In *a*, solid chain segments show regions in contact with the NC41 antibody; contact assignments in the broken solid segments are tentative.

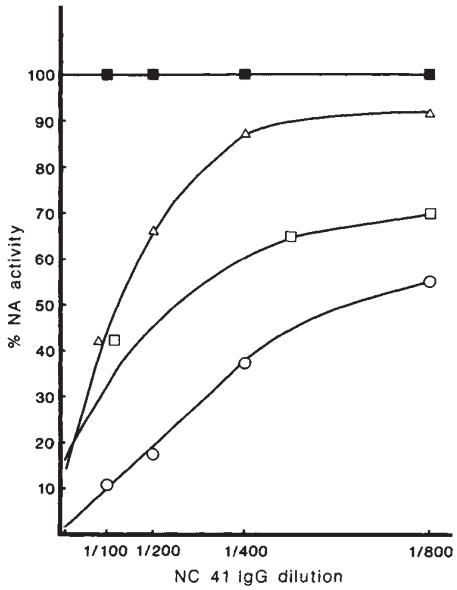

Fig. 2 Neuraminidase inhibition (NI) curves of monoclonal antibody NC41 acting on N9 neuraminidase (NA) and a number of variants selected with different monoclonal antibodies to N9 neuraminidase. Assays used fetuin as a substrate, as described[58]. The amino-acid sequence changes of the variants are: ■, 434 (432 in N2 numbering) K→N; 400 (400) N→K; 371 (370) S→L; 370 (369) A→D; 368 (367) S→N; □, 369 (368) I→R; △, 331 (329) N→D (designated as OX2 in text); ○, 222 (220) R→Q (this curve is identical to wild-type). The amino-acid sequence changes were determined by sequencing cDNA of the viral RNA strand encoding the neuraminidase as described[59]. The changes are shown on the 3-D structure of the monomer in Fig. 1.

describing the angle between the local axes of symmetry in the V and C modules.

The identification of antigenic regions on protein molecules[19] has been attempted by a variety of methods[20–23] but the structural basis of antigenicity remains unclear. Current models of antigen–antibody association are based on classical ideas of lock and key complementarity. But it has been suggested[24] that the antigenic regions of proteins are located in the more flexible chain segments, which may adopt a configuration that allows antibody binding. It is not known whether binding to antigen has any effect on the structure of an antibody[25], nor whether, if such an effect exists, it has biological significance. For the Fab–lysozyme complex[12], the parts of the lysozyme that make contact with the antibody are not the more flexible regions of free lysozyme. No deformation of the antigen nor any structural change in the Fab was observed[12].

The antigen in this study is the neuraminidase of influenza virus. It is a tetramer of subunits with relative molecular mass 60,000 (M_r 60 K) with circular symmetry, and is attached by a stalk to the viral membrane. Neuraminidase 'heads' can be liberated from the virus by proteolysis[26]. There is antigenic variation in the neuraminidase between different strains of virus. Antibodies against neuraminidase do not neutralise virus infectivity, but do modify the disease in favour of the host[27]. The three-dimensional structures of neuraminidase heads of subtypes[28] N2 (refs 29, 30) and N9 (A.T.B., J.N.V., W.G.L., G.M.A. and P.M.C., manuscript in preparation) are known and a schematic of the chain fold is shown in Fig. 1. Neuraminidase of subtype N9 from an avian influenza virus, G70c[31], has been used in this study. Its structure is very similar to the N2 enzyme as expected from the sequence homology of 50% (ref. 32).

We previously reported electron and low resolution X-ray diffraction studies of Fab-neuraminidase complexes[33] and, more recently, the crystallization of another complex (with NC41 Fab) which diffracts X-rays to beyond 3 Å resolution[34]. The NC41 antibody can suppress the yield of virus from infected cells and therefore allows the selection of antigenic variants. Neuraminidase-inhibition curves (Fig. 2) show that some variants with single sequence changes are not inhibited at all by NC41 antibody whereas others are partially inhibited. The location of these sequence changes on the three-dimensional structure of neuraminidase is shown in Fig. 1.

Protomer structure

Electron microscopy of negatively stained protomers of complex show tetrameric neuraminidase heads with four Fab fragments attached (data not shown). Their image appearance is very similar to that of protomers of N9 neuraminidase complexed with the Fab fragments of antibodies 32/3 and NC35 (ref. 33) and may be described as a square box (100×100×60 Å) with four antennae (Fab molecules) attached to one surface on the outer corners. The overall shape of the protomer from the X-ray diffraction study (Fig. 3) is consistent with the electron microscope images. The Fab arms subtend an angle of 45° to the plane of the tetrameric neuraminidase head, slightly foreshortened in the electron microscope image[33].

Surface loops of the neuraminidase in contact with the CDRs are 368–370, 400–403, 430–434 and parts of 325–350. Of these, the conformation of the 325–350 loop is still tentative. It was the most difficult region of the original N2 neuraminidase structure[29] to interpret and remains ambiguous in the N9 neuraminidase structure (A.T.B. *et al.*, manuscript in preparation). Such instances of ill-defined structure are typical of surface loops of polypeptides subject to thermal motion or statistical disorder.

Early indications on the distribution of temperature factors in the uncomplexed N2 neuraminidase, based on crystallographic refinement of that structure at 2.2 Å resolution and an *R*-factor of 0.293, show above-average thermal parameters in chain segments 109–111, 141–142, 221–222, 243–247, 305–309, 316–319, 327–331, 338–343, 365–369, 399–402, 429–437 and 461–469 (J.N.V. and P.M.C., unpublished data). Elevated *B* values around residue 330 may correlate with inaccurate modelling as discussed above. All the segments listed here are surface loops. Note that only one of the hotter loops is underneath the neuraminidase head. We emphasize that the temperature factor analysis is preliminary, and indeed relates to N2, not N9, neuraminidase.

The monoclonal variant of N9 neuraminidase known as OX2 (Asn 329→Asp 329, N2 numbering) crystallizes isomorphously with wild-type N9–NC41 Fab complex[34]. NC41 inhibits the OX2 neuraminidase variant less than it does wild-type (Fig. 2). Refinement of the N9–NC41 Fab structure using data collected from the OX2-NC41 Fab complex yields an *R*-factor of 0.36 for a model with tight geometry. This result is comparable with the current *R*-factor against the native dataset and confirms our earlier conclusion[34] that the binding of NC41 Fab to wild-type and OX2 N9 neuraminidases is isosteric. Either some bonding 'glue' is absent or repulsive forces have been introduced by the mutation (Fig. 2), but there is no detectable rearrangement of the antibody on the antigen at this stage. The precise location of residue 329 (N2 numbering) in the N2 and N9 structures is unclear. Refinement of the OX2-NC41 Fab structure should eventually reveal the structural basis for the reduced binding of NC41 to OX2 compared with wild-type N9.

The third CDRs on both heavy and light chains are not yet completely modelled, and the conformation of the 325–350 region on the antigen remains uncertain, so we cannot identify the amino acids that interact in the interface. All the CDRs, with the possible exception of light-chain CDR1 appear to make contact with the epitope. A preliminary assessment is that there are no more contacting residues than the 16 or 17 observed in the Fab–lysozyme structure[12].

Quaternary structure of the Fab

The amino-acid sequence of the Fab is known (G.M.A., unpublished data). The assignment of heavy and light chains in the Fab structure is consistent with side-chain densities at homologous positions on the two chains, such as heavy-chain (H) Trp 47 and light-chain (L) Leu 46, H Val 37 and L Tyr 36, and, H Trp 103 and L Phe 98. Heavy-atom binding sites also show an asymmetry which is consistent with these observations.

The quaternary structures of known Fab fragments were compared as described in Table 1. The lower left triangle of entries indicates that C_L-C_{H1} pairing is a function of immunoglobulin chain subtype since $\gamma_1:\lambda$ chains (as in Kol and New) show a consistent mode of association as do α or $\gamma_{2a}:\kappa$ chains (as in M603 and NC41). Small but significant alterations in V-domain pairing are observed between Kol, New and M603 (Table 1, upper right). This variation in V_L-V_H association has been attributed to the fact that the CDRs contribute partially to the dimer interface between the two domains in the V-module[14], although in the case of Kol we suggest that intimate crystal contacts involving the CDRs may contribute.

Comparison of these three Fabs with NC41 complexed with neuraminidase shows, in each case, a significantly larger difference in V_L-V_H association. Compared with Kol, the distance between H CDR2 and L CDR3 is larger and the relative positions of the CDRs around the antigen-binding surface are altered by up to 4 Å. A movement of this magnitude is of the order of the distance between adjacent α-carbon atoms on a polypeptide and may be considered as dramatic as a sequence insertion or deletion in a structurally critical part of the molecule. As well as the bulk movement of domains described here, the CDR loops may be flexible and able to adapt further to an epitope.

Building an atomic model into the penultimate electron density map (that in which no phase information from the Fab structure had been included) required the rotation of H Trp 47 180° around C_α-C_β compared with its position in Kol. M603 and New are the same as Kol at this point. The positions of the loops at residue 40 on both heavy and light chains also required remodelling. Therefore the reorganization of the interface through sliding of domains has consequences for the domain structure of the V_L and V_H.

The sequence of the NC41 V_L and V_H domains shows that those framework amino acids on both the light chain (Tyr 36, Gln 38, Pro 44, Tyr 87, Phe 98) and the heavy chain (Val 37, Gln 39, Leu 45, Trp 47, Phe 91, Ala 93, Trp 103) that are buried in the interface[15] are conserved as expected. There is nothing in the primary sequences of the CDRs of NC41 to suggest a cause of the unusual domain association. An independent analysis of the NC41 sequence confirms this view (C. Chothia, personal communication).

Two other Fab structures are known to fit the normal pattern of V_L-V_H association, the free antineuraminidase monoclonal antibody S10/1 (ref. 11) and the complexed anti-lysozyme monoclonal antibody D1.3 (ref. 12). Among light-chain dimers the picture is less clear. Although several examples of V_L-V_H-like association have been observed[3,35-37], there are two clear exceptions[38-39], one of which is said to be caused by the CDR residue L 91, or, in our view, perhaps by a His at residue 38.

If changes in the amino-acid sequence of the CDRs (which are only a small part of the interface) can modulate the pairing pattern, binding of the six CDRs to a macromolecular surface might similarly perturb the V_L-V_H interface. Without knowing the three-dimensional structure of the free NC41 Fab we cannot definitely conclude that the antibody structure has changed on binding antigen, but we believe that this explanation is more plausible than the alternative, which requires that special sequences in the CDRs alone have determined the pairing pattern.

Other data support conformational changes in antibodies when antigen or hapten binds[40-44]. Changes in circular dichroism[40] or circular polarization of fluorescence[42] indicate an altered environment for aromatic residues after antigen binds to antibody, and kinetic data support a bi-molecular process with distinct conformational states for bound and free Fab[41,43,44]. Both of these aspects are embodied in the sliding V_L-V_H model presented here.

Direct structural evidence has been presented for hapten-induced structural changes in a Bence-Jones protein[45,46]. In that case hydrophobic ligands can apparently penetrate the V_L-V_L interface and signal their presence to the C-module. Strain introduced in the structure of the C-module can be relaxed by reducing and re-oxidizing the disulphide bond between the C-terminal regions of the two light chains[46]. Table 1 indicates that in the neuraminidase-NC41 complex no significant changes in the quaternary structure of the C-module have occurred.

Analysis of the pseudo-symmetry axes of the V and C modules shows that the angle between these axes, the elbow angle, is ~150°, which is intermediate in the observed range of 130–180° for other Fab structures. The sense of the bending is the same as in all other Fab fragments, with V_H and C_{H1} domains closer together than the V_L and C_L domains.

Table 1 Quaternary structure comparisons of Fabs

	NEW	M603	KOL	NC41
NEW		4.2 (0.7)	6.5 (0.4)	12.2 (1.0)
M603	12.7 (2.3)		5.0 (0.3)	8.8 (1.3)
KOL	2.5 (0.0)	12.4 (2.4)		12.1 (0.7)
NC41	11.5 (0.4)	2.1 (0.7)	10.8 (2.1)	

Comparison of four different Fab quaternary structures. Upper right triangle: V_L domain of the row Fab was mapped into the V_L domain of the column Fab using the C_α coordinates of residues 33–39, 43–47, 84–90, 98–104 (Kabat[2] numbering). These amino acids were chosen because they define the interface between V_L and V_H domains[15]. The calculated transformation was applied to the V_H domain of the row Fab and the additional rotation in degrees (and translation in Å) to optimize overlap of the two V_H domains in question was calculated and is given above. C_α coordinates used for overlap of V_H domains were 34–40, 44–48, 88–94 and 103–109. Lower left triangle: C_L domain of the column Fab was mapped into the C_L domain of the row Fab using the C_α coordinates of residues 118–124, 131–137, 160–162 and 174–178 (Kabat[2] numbering). These amino acids were chosen because they define the interface between C_L and C_{H1} domains[16]. The calculated transformation was applied to the C_{H1} domain of the column Fab and the additional rotation in degrees (and translation in Å) to optimize overlap of the two C_{H1} domains are shown. C_α coordinates used for overlap of C_{H1} domains were 121–125, 139–145, 172–179 and 186–190. Amino acids from the interface were used because if this set is expanded to include other parts of the domain structure, the correlation between small rotation angles and similar chain classes that is observed for the C module is less good. The largest r.m.s. distance between domain structure alignments is 0.7 Å. A similar comparison was done for the V modules of the M603 (antiphosphocholine) and uncomplexed S10/1 (antineuraminidase) Fab fragments. No measurable difference in the way the V_L and V_H domains associate in those antibodies was detected. A comparison elsewhere of Kol and New V modules[8] yields a value of 9°. The value reported here (6.5°) is smaller because it is uninfluenced by structural differences outside of the interface zone.

Conformational changes in the antigen

The neuraminidase upper surface loop involving residues 367–371 was remodelled to better fit the density as observed in the complex. Adjacent parts of the loop which were also omitted from the phasing process (residues 364–366 and 372–373) fit the density as if they are rigidly attached to the N9 core. The C_α atoms of residues 368–371 have been moved by 1 Å or more from their position in N9 neuraminidase (Fig. 4). Least-squares refinement of the structure to $R = 0.35$, gave a mean shift of 0.4 Å in all C_α atoms with a standard deviation of 0.2 Å. The current position of the 370 loop (Fig. 4) shows displacements of more than 1.2 Å for C_α atoms 369–371 compared with their

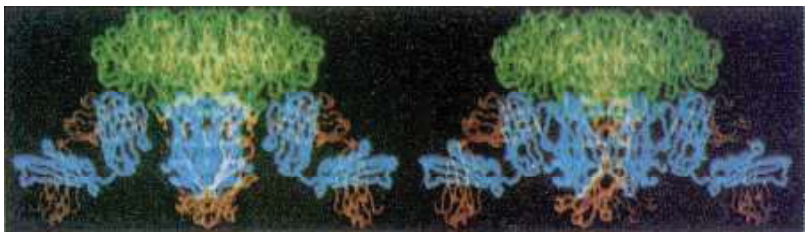

Fig. 3 Stereo images of the C_α skeleton of the protomer, showing four Fab molecules attached to one tetrameric neuraminidase 'head'. Neuraminidase, purple; heavy chain, green; light chain, blue. View with the protomer 4-fold axis vertical, but tipped towards the viewer. The crystals of N9-NC41 Fab belong to the space group $P42_12$ with $a = 167$ Å, $c = 124$ Å (ref. 34). There is one quarter of a protomer per asymmetric unit and 70% of the cell volume is occupied by solvent. Data were collected photographically to 3 Å resolution. In all, 67,976 measurements of 25,241 independent reflections, representing 76% of the data in the 3 Å sphere, were merged with an *R*-factor on intensities of 0.12. Phasing was initiated through two heavy atom derivatives (potassium tetra-chloro-platinate and diamino-dinitro-platinum). An envelope was computed[60] on the basis of a 5 Å resolution electron-density map allowing the location of the neuraminidase tetramer on the crystallographic 4-fold axis to be determined first by inspection and subsequently by correlation methods in real space and rigid body least-squares refinement[61], resulting in a correlation coefficient of 0.204 between F_{obs} and F_{calc} for data in the range 5–3.5 Å. It was now clear which surface regions of the neuraminidase were in contact with the remaining electron density in the image, and, in subsequent use of neuraminidase as partial structure in the phasing process, those regions were excised. A second electron density map, now at 3.5 Å resolution, was phased on the two derivatives (one to 5 Å and one to 3.5 Å), the neuraminidase partial structure, and solvent flattening from a redetermined envelope. The four domains of the Fab fragment were recognised in this map and fitted independently by real-space correlation methods with the known Fab structure Kol[8]. Rigid-body least-squares refinement with five groups, neuraminidase, V_H, C_{H1}, V_L and C_L produced shifts of up to 1.5° in group orientations and led to an R-factor of 0.425 and a correlation coefficient of 0.308 for data between 5 and 4 Å resolution. The structure is based on a 3 Å electron density map, which is phased in addition to the information listed above with the structure of the Fab fragment excluding the complementarity-determining loops. Thus there is no structural prejudice in the image of those parts of the antigen or antibody that are near, or in, the bonding interface. Further refinement[62] has since reduced the residual to 0.35 for data between 6 and 3 Å resolution. The r.m.s. error in the atomic positions is of the order of 0.5 Å at this stage.

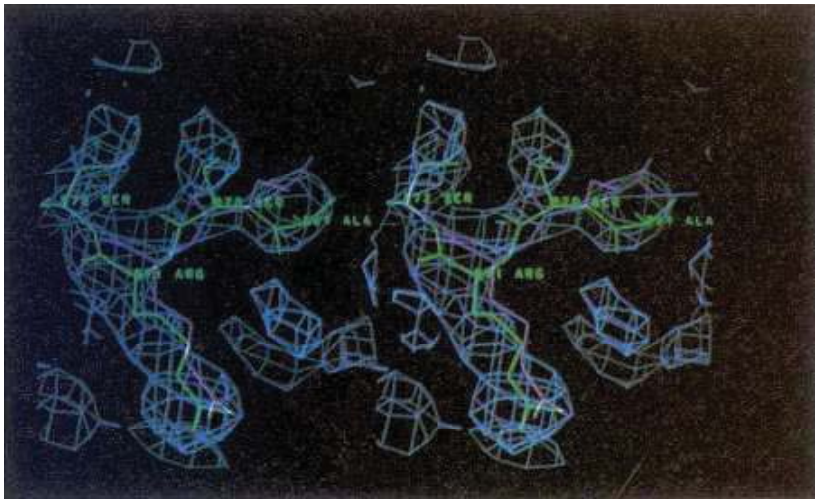

Fig. 4 Stereo image of the electron density map (2Fo–Fc, $R = 0.35$) of the neuraminidase loop 368–372 in the complex with NC41 Fab. Residues here are labelled 868–872. The yellow model shows the current fit of the loop in the complex structure. The purple model is the position of this loop in uncomplexed N9 neuraminidase.

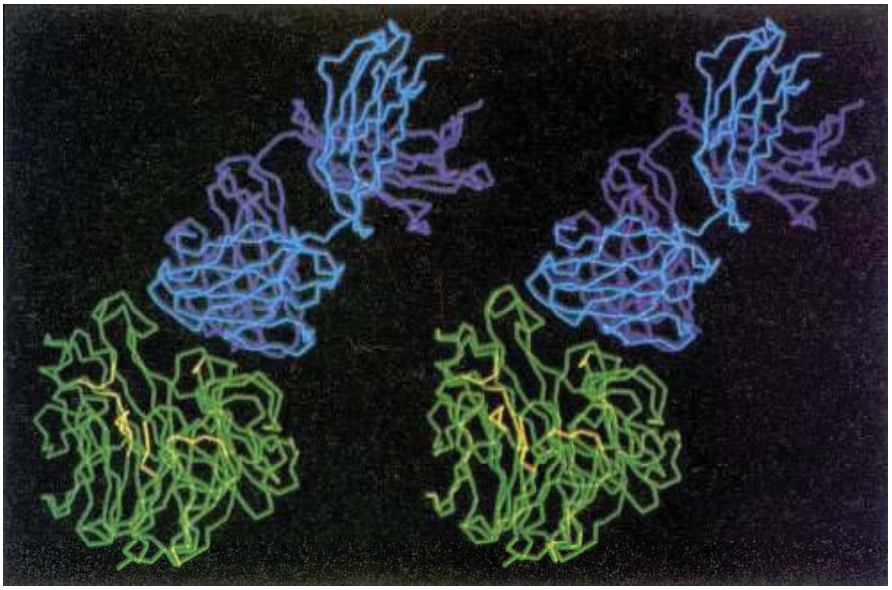

Fig. 5 Stereo image of one quarter of the protomer, showing the Fab bound to the side of the active site cavity on the enzyme. The enzyme active centre is facing the viewer, below and to the left of the antibody binding site, and is coloured yellow. The neuraminidase perspective is as in Fig. 1*b*. Neuraminidase, green; heavy chain, purple; light chain, blue.

position in free N9 neuraminidase. Thus the antigen is distorted by interaction with the antibody.

Most monoclonal anti-neuraminidase antibodies inhibit neuraminidase activity against fetuin, but only some of these also inhibit activity against the trisaccharide sialyl-lactose[47]. Although NC41 Fab cannot sterically block entry of a trisaccharide into the active site (Fig. 5), NC41 does inhibit this activity (R.G.W., manuscript in preparation). We suggest that one possible mechanism for enzyme inactivation is the small displacement of Arg 371, which points directly into the catalytic site. We cannot yet rule out other interpretations, such as the effect of the antibody on steering substrates and products into or out of the active site. It has been shown that changing Arg 371 for Lys by site-specific mutagenesis results in the loss of 90–95% of enzyme activity, although the mutated protein is correctly folded (M. R. Lentz, R.G.W. and G.M.A., manuscript in preparation).

Deformation of antigens by antibodies has been proposed to explain a variety of experimental data, including single-hit kinetics for neutralization of polio virus[48] and altered binding affinity for second antibodies binding noncompetitively to the antigen[49]. The capacity of anti-apomyoglobin antibodies to, effectively, expel the haem from myoglobin has long been known[50]. There are also many reports of antibodies inhibiting enzymes[51]. Our results directly demonstrate that conformational changes can be induced in antigens by antibodies. Furthermore, the change observed here, although small, correlates with the inactivation of the neuraminidase towards sialyl-lactose. Other anti-neuraminidase antibodies that inhibit neuraminidase activity only towards large substrates and, like NC41, can select antigenic variants, probably inhibit enzyme activity by blocking access of large substrates to the active site. We are testing the hypothesis that such antibodies do not distort the active site of the enzyme by an X-ray diffraction study of the N9-NC10 Fab complex[34]. Unlike NC41, this antibody does not inhibit enzyme activity on sialyl-lactose. Antigen distortion is likely to be but one of a number of possible mechanisms for virus neutralization[52].

Conclusions

The structure of a complex between an antibody and influenza virus neuraminidase shows features inconsistent with a rigid 'lock and key' model for antibody–antigen interactions. In contrast to the findings from a lysozyme–antibody complex[12] we observe (1) an unusual V_L–V_H pairing in the V module of the Fab, and (2) local perturbation of the antigen at the centre of the epitope. The interaction therefore has some of the character of a handshake. NC41 Fab has not yet been crystallized, and we can only suppose on the basis of sequence data that its structure is similar to the common pattern among all six other Fab structures in the literature. We propose that, during antigen binding, the V_L and V_H domains of the antibody slide at their interface. The extent of sliding is small, but sufficient to move the CDRs by at least 3 Å. If such a structural transition has occurred, it is presumably of low energy and therefore low cost to the binding affinity for the antigen. The observation that V_L–V_H dimers associate in a way not found in associations of other β-sheet structures has led to the suggestion that this novel association might produce static or dynamic properties important for antigen binding[13]. The ability of domains to slide could expand the range of specificities of a single antibody species. Cross-reactivity of monoclonal antibodies with proteins unrelated to the immunizing antigen[53] could occur by different extent, or direction, of domain sliding.

Diversity of antibody specificities is generated by libraries of germline gene sequences, by somatic events and by combination of different H and L chains[54]. If the V module can generate diversity through V_L–V_H sliding, this presents yet another mechanism for fine-tuning the specificity of an antibody. We do not suggest that all antigen–antibody interactions will involve reorganization of the V_L–V_H interface. The lysozyme–Fab complex[12] apparently does not. Thus the only biological significance we attach to V_L–V_H sliding is that, in some instances, it may facilitate the formation of a functional immune complex.

A necessary, but apparently insufficient, condition to induce sliding is the interaction of the epitope with CDRs from both H and L chains. It may be that the larger radius of curvature of neuraminidase, compared with lysozyme, restricts the capacity of the Fab to bind in its ground state.

Sequence data on the T-cell receptor are consistent with the α- and β-chains being immunoglobulin-like[55,56]. We note further that those sequences contain the characteristics of V_L and V_H sequences that have been attributed to the novel association of V_L and V_H domains[15]. If the principles of recognition of antigens by T- and B-cell receptors are indeed similar[57], then induced fit of antigen to receptor might also be a feature of cellular immunity.

As the two reported antigen–antibody complex structures are rather different, more data on similar systems are required to establish the importance of V_L–V_H sliding to immune recognition.

We thank Paul Davis for computing assistance, Bert van Donkelaar and Janet Newman for technical assistance, Cyrus Chothia for communicating results in advance of publication and the Australian Overseas Telecommunications Commission for donating international dialling facilities. Some of the OX2–NC41 data were collected at SSRL and we thank Paul Phizackerly for assistance. This work was supported by the US National Institutes of Health.

Note added in proof: The NC41 V_H belongs to the recently characterized V_H family IX (Winter, E., Radbuch, A. and Krawinkel, V. *EMBO J.* **4**, 2861–2867 (1985)).

Received 11 November 1986; accepted 3 February 1987.

1. Colman, P. M. & Ward, C. W. *Curr. Top. Microbiol. Immun.* **114**, 178–255 (1985).
2. Kabat, E. A., Wu, T. T., Bilofsky, H., Reid-Miller, M. & Perry, H. *Sequences of Proteins of Immunological Interest* (US Department of Health and Public Services, Washington DC, 1983).
3. Schiffer, M., Girling, R. L., Ely, K. R. & Edmundson, A. B. *Biochemistry* **12**, 4620–4631 (1973).
4. Poljak, R. J. *et al. Proc. natn. Acad. Sci. U.S.A.* **70**, 3305–3310 (1973).
5. Segal, D. M. *et al. Proc. natn. Acad. Sci. U.S.A.* **71**, 4298–4302 (1974).
6. Matsushima, M. *et al. J. molec. Biol.* **121**, 441–459 (1978).
7. Saul, F., Amzel, L. M. & Poljak, R. J. *J. biol. Chem.* **253**, 585–597 (1978).
8. Marquart, M., Deisenhofer, J., Huber, R. & Palm, W. *J. molec. Biol.* **141**, 369–392 (1980).
9. Satow, Y., Cohen, G. H., Padlan, E. A. & Davies, D. R. *J. molec. Biol.* **190**, 593–604 (1986).
10. Suh, S. W. *et al. Proteins: Structure, Function and Genetics*, **1**, 74–80 (1986).
11. Colman, P. M. & Webster, R. G. in *Biological Organisation: Macromolecular Interactions at High Resolution* (ed. Burnett, R.) 125–133 (Academic, New York, 1987).
12. Amit, A. G., Marriuzza, R. A., Phillips, S. E. V. & Poljak, R. J. *Science* **233**, 747–753 (1986).
13. Novotny, J. & Haber, E. *Proc. natn. Acad. Sci. U.S.A.* **82**, 4592–4596 (1985).
14. Davies, D. R., Padlan, E. A. & Segal, D. M. *A. Rev. Biochem.* **44**, 639–667 (1975).
15. Chothia, C., Novotny, J., Bruccoleri, R. & Karplus, M. *J. molec. Biol.* **186**, 651–663 (1986).
16. Padlan, E. A., Cohen, G. H. & Davies, D. R. *Molec. Immun.* **23**, 951–960 (1986).
17. Colman, P. M., Deisenhofer, J., Huber, R. & Palm, W. *J. molec. Biol.* **100**, 257–282 (1976).
18. Davies, D. R. & Metzger, H. *A. Rev. Immun.* **1**, 87–117 (1983).
19. Benjamin, D. C. *et al. A. Rev. Immun.* **2**, 67–101 (1984).
20. Crumpton, M. J. & Wilkinson, J. M. *Biochem. J.* **94**, 545–556 (1965).
21. Smith-Gill, S. J. *et al. J. Immun.* **128**, 314–322 (1982).
22. Lerner, R. A. *Nature* **299**, 592–596 (1982).
23. Tainer, J. A. *et al. Nature* **312**, 127–134 (1984).
24. Westhof, E. *et al. Nature* **311**, 123–126 (1984).
25. Metzger, H. *Contemp. Top. molec. Immun.* **7**, 119–152 (1978).
26. Laver, W. G. *Virology* **86**, 78–87 (1978).
27. Schulman, J. L. in *The Influenza Viruses and Influenza* (ed. Kilbourne, E. D.) 373–393 (Academic, New York, 1975).
28. Webster, R. G., Laver, W. G. & Air, G. M. in *Genetics of Influenza Viruses* (ed. Palese, P. & Kingsbury, B. W.) 127–168 (Springer, New York, 1983).
29. Varghese, J. N., Laver, W. G. & Colman, P. M. *Nature* **303**, 35–40 (1983).
30. Colman, P. M., Varghese, J. N. & Laver, W. G. *Nature* **303**, 41–44 (1983).
31. Laver, W. G., Colman, P. M., Webster, R. G., Hinshaw, V. S. & Air, G. M. *Virology* **137**, 314–323 (1984).
32. Air, G. M., Ritchie, L. R., Laver, W. G. & Colman, P. M. *Virology* **145**, 117–122 (1985).
33. Tulloch, P. A. *et al. J. molec. Biol.* **190**, 215–225 (1986).
34. Laver, W. G., Webster, R. G. & Colman, P. M. *Virology* **156**, 181–184 (1987).
35. Epp, O. *et al. Biochemistry* **14**, 4943–4952 (1975).
36. Epp, O. *et al. Eur. J. Biochem.* **45**, 513–524 (1974).
37. Colman, P. M., Schramm, H. J. & Guss, J. M. *J. molec. Biol.* **116**, 73–79 (1977).
38. Furey, W., Wang, B. C., Yoo, C. S. & Sax, M. *J. molec. Biol.* **167**, 661–692 (1983).
39. Chang, C. H. *et al. Biochemistry* **24**, 4890–4897 (1985).
40. Holowka, D. A., Strosberg, A. D., Kimball, J. W., Haber, E. & Cathou, R. E. *Proc. natn. Acad. Sci. U.S.A.* **69**, 3399–3403 (1972).
41. Levison, S. A., Hicks, A. N., Portman, A. J. & Dandliker, W. B. *Biochemistry* **14**, 3778–3786 (1975).

DOCKET ALARM

Explore Litigation Insights

Docket Alarm provides insights to develop a more informed litigation strategy and the peace of mind of knowing you're on top of things.

Real-Time Litigation Alerts

Keep your litigation team up-to-date with **real-time alerts** and advanced team management tools built for the enterprise, all while greatly reducing PACER spend.

Our comprehensive service means we can handle Federal, State, and Administrative courts across the country.

Advanced Docket Research

With over 230 million records, Docket Alarm's cloud-native docket research platform finds what other services can't. Coverage includes Federal, State, plus PTAB, TTAB, ITC and NLRB decisions, all in one place.

Identify arguments that have been successful in the past with full text, pinpoint searching. Link to case law cited within any court document via Fastcase.

Analytics At Your Fingertips

Learn what happened the last time a particular judge, opposing counsel or company faced cases similar to yours.

Advanced out-of-the-box PTAB and TTAB analytics are always at your fingertips.

API

Docket Alarm offers a powerful API (application programming interface) to developers that want to integrate case filings into their apps.

LAW FIRMS
Build custom dashboards for your attorneys and clients with live data direct from the court.

Automate many repetitive legal tasks like conflict checks, document management, and marketing.

FINANCIAL INSTITUTIONS
Litigation and bankruptcy checks for companies and debtors.

E-DISCOVERY AND LEGAL VENDORS
Sync your system to PACER to automate legal marketing.